Simulation of a Scintillator-based Compton telescope with micropattern readout

Robert. L. Varner and James. R. Beene

***Abstract*—We describe simulations of a Compton telescope gamma-ray detector. The model is based on scintillation detectors and low-mass, photosensitive micro-pattern detectors, particularly the plasma panel sensor. The detector model has ten to twenty layers, to maximize the probability of Compton scattering while minimizing multiple scattering in a single layer. The simulations explore optimizing the micro-pattern detector pixel geometry, the scintillator material, the total detector thickness, and the number of layers. In addition, we explored algorithms for determining the interaction position, total energy and discriminating Compton scattering from other processes. Our initial results indicate that this kind of Compton telescope can be much more efficient that silicon or germanium-based telescopes while providing very good position resolution.**

I. Introduction

THE Plasma Panel Scintillation Detector (PPSD)[1] is a new idea in micropattern detectors. It is a modified plasma display panel, used as a large array of microscopic discharge cells. The cells are filled with gases in high electric fields awaiting ionization to trigger a discharge. In the PPSD, a photoemissive layer is introduced into each cell, so that incident photons can generate electrons needed to trigger a discharge. The cells are small, between 10μm to 100μm in diameter with a recovery time less than 1μs. The panel can be very efficient, because each cell has a very high gain of about 10^{11}, yet it is of low mass, being only 1 to 10 mm thick. Because of the avalanche discharge, we get no energy information from individual cell discharges. Instead, the number and location of the discharges provide energy and position information. Design optimization will determine the required threshold for scintillation photon detection, the required pixel size and spacing for optimum position and energy resolution, and the maximum mass of detector material that can be tolerated between layers.

This paper describes the ideas behind a Compton telescope array and our initial simulations to demonstrate how a scintillator-PPS based array will perform in terms of position resolution, energy resolution and efficiency.

Manuscript received November 8, 2007. Prepared by Oak Ridge National Laboratory, P.O. Box 2008, Oak Ridge, Tennessee 37831-6285, managed by UT-Battelle, LLC, for the U.S. Department of Energy under contract DE-AC05-00OR22725.

Physics Division Oak Ridge National Laboratory, P. O. Box 2008, Oak Ridge, TN 37831 USA

II. Compton Telescope

A Compton telescope is a sequence of detectors using Compton scattering to deduce the energy and angle of incidence of a γ-ray. Such detectors have been used in space-based gamma-ray detectors[2], and are being considered for a number of terrestrial applications, including biomedical imaging[5]. Compton scattering of a gamma-ray from the electrons in a material induce a change in the photon wavelength which is related to the angle of the scattering,

$$\cos\phi_1 = 1 - m_e c^2 \left(\frac{1}{E_1} - \frac{1}{E_0}\right)$$

where E_0 is the incident photon energy, E_1 is the photon energy after scattering, ϕ_1 is the angle at which the photon scatters and $m_e c^2$ is the rest mass energy of the electron. Comparing the incident energy and the scattered energy can give the scattering angle. A variation of this technique is the "3-Compton technique" [2] in which two successive Compton scatterings are detected following from the same incident γ, followed by a third detection of any kind of interaction (photoelectric effect, Compton scattering or pair production).

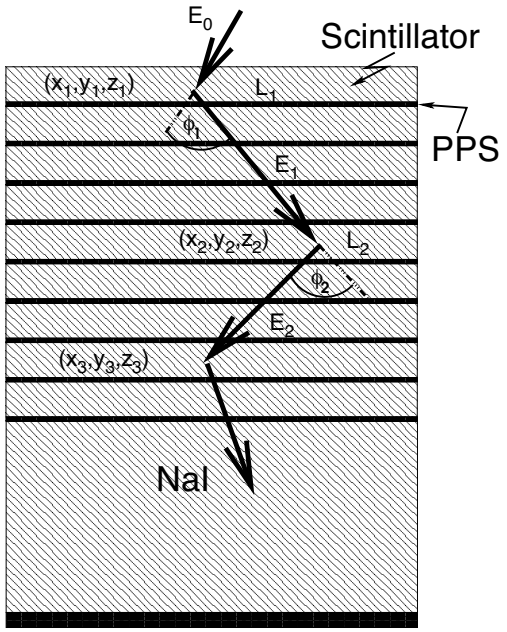

Fig. 1. Schematic of the PPS-based Compton telescope

One measures only L_1, the energy deposited in the first scatter, L_2, the energy deposited in the second scatter, and ϕ_2, the scattering angle of the second scatter. The positions, (x_n, y_n, z_n) are determined in order to compute the angle. Use

of these two scatterings eliminates the need for an accurate measure of the total energy,

$$E_0 = L_1 + \frac{L_2}{2} + \frac{1}{2}\left[L_2^2 + \frac{4m_e c^2 L_2}{1-\cos\phi_2}\right]^{\frac{1}{2}}$$

from which

$$\cos\phi_1 = 1 - m_e c^2\left(\frac{1}{E_0 - L_1} - \frac{1}{E_0}\right)$$

is calculated.

The determination of ϕ_1 does not immediately pinpoint the source of the γ-ray. The angle determines the surface of a cone on which the source is located. The sources are located by combining a large number of γ-ray events and examining where all the resulting cones intersect.

To design an effective Compton telescope, we need to optimize several parameters. We must have sufficient energy resolution, good position resolution, and high efficiency with γ-ray interactions in the detectors dominated by Compton scattering. The energy deposited in each Compton scatter can be small compared to the energy of the incident photon. We must minimize the number of multiple interactions in a layer, since these are difficult to distinguish from single interactions and confuse the subsequent analysis. We also need to identify the order in which scattering occurs, not always simple since backscattering is possible.

From these relations, precision in the energy measurements L_1 and L_2, and precision in the positions of the three scatterings, from which we determine ϕ_2 are most important in the determination of the initial scattering angle. It is also important to have high detection efficiency since many events are required to identify uniquely the source location.

III. Detector material, layer thickness and total thickness

We began by making simple estimates of interactions from gamma-ray linear attenuation coefficients, over a reasonable range of gamma energies, 0.1 to 10 MeV. We investigated NaI and plastic scintillator as the scintillator material. The choice of scintillator material to be used requires some compromises. Examining Table 1, one can see that a Compton telescope based upon plastic scintillator requires three to five times the thickness of material required by a telescope of NaI. Sodium iodide also has the advantage of emitting four to five times as many optical photons for the same interaction as plastic scintillator, giving a much improved energy resolution. Plastic scintillator has the advantage that nearly all the scattering in the energy range we care about is Compton scattering, unlike NaI which has significant contributions from photoelectric absorption below 1 MeV. Photoelectric absorption events reduce our efficiency and confuse our signal processing. While the ideal detector will be composed of some mixture of plastic and NaI, or based on high light output, lower-Z materials, we chose to base these preliminary simulations on a more compact NaI telescope.

The thickness of the individual detector layers is determined by our desire to keep the number of non-Compton-scattering events small, and the number of multiple Compton-scattering events in a layer as close to zero as possible. We used tabulated linear attenuation coefficients [3] for NaI to estimate the probability of single scatters and maximizing this compared to the probability for more than one scattering event. The result is in Table 1.

TABLE I
Required scintillator layer thickness, t_1, from linear attenuation data. This choice of thickness gives a 25% probability for a single Compton scattering, 70% probability of no interaction, and 5% probability of more than one-interaction. Also in the table are the required thicknesses to get 2 or more Compton scatters ($t_{\geq 2}$) and 3 or more, $t_{\geq 3}$. The column labeled $\mu(cm^{-1})$ is the linear attenuation coefficient for the material and energy specified.

E(MeV)	$\mu(cm^{-1})$	t_1(cm)	$t_{\geq 2}$(cm)	$t_{\geq 3}$(cm)
NaI				
0.66	0.26	1.4	18.	24.
1.0	0.20	1.8	24.	32.
2.0	0.15	2.4	32.	42.
3.0	0.14	2.6	34.	45.
5.0	0.12	2.9	40.	53.
Plastic Scintillator BC400				
0.66	0.080	4.5	59.	79.
1.0	0.070	5.1	68.	90.
2.0	0.048	7.4	99.	131.
3.0	0.039	9.1	122.	162.
5.0	0.027	13.1	176.	233.

Another critical design parameter is the total detector thickness. If we want to maximize the efficiency of the telescope for detecting γ-rays, we need enough thickness to have a high probability for three-hits in the assembly. In the version of the

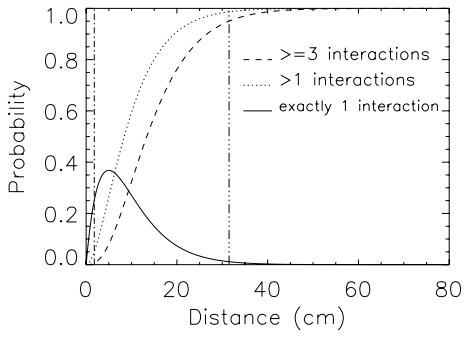

Fig. 2. Selection of optimal single layer thickness and total thickness for E_γ of 1 MeV in NaI. The vertical line near Distance = 1 cm defines t_1, which determines the optimum layer thickness and the line at large distance defines $t_{\geq 3}$, which determines the total detector thickness

detector we modeled, we used a very thick absorption layer in back of the telescope to guarantee a third hit for either NaI or plastic. Because of this back layer, we could experiment with relaxing the requirement of three or more scatters to two or more scatters in our design, if the position resolution in the thick layer is sufficient. The thickness required for two-or-more scatters, $t_{>2}$ is also shown in Table 1.

Optimizing the detector for the entire range of energies of interest suggests that we adopt a layer of NaI, 0.5 to 2 cm thick for each element, to optimize our single-hit probability for low energy γ-rays, with 10 to 20 elements, to give us enough total thickness for the high-energy γ-rays.

The information we hope to obtain from the PPS includes precise positions in three dimensions of the Compton scattering interactions and the energy deposited in the interaction. The PPS is unusual, because it has many small pixels which respond as binary elements to incident photons. The recovery time of the pixels, 1μs, makes the PPS blind to multiple hits from NaI photons in the same event.

Our simulation of the position readout was based on finding the centroid in (x,y) of the distribution of pixels which fire in each event. NaI produces about 4×10^4 photons/MeV of incident gamma-ray energy. The energy resolution of the layer depends on the number of these photons we detect in the PPSD. The number we detect depends on the quantum efficiency of the detector, the threshold for observing the photoelectron, the geometric acceptance of the PPS and the efficiency of the optical coupling between the two devices. We assumed a quantum efficiency of 25%. We simulated a black-faced scintillator, so that only photons directly impinging on the PPS would contribute. The density of the photons is cylindrically symmetric about the perpendicular from the PPSD to the scatter event. The distribution function is proportional to $\cos^2\theta$ where θ is the angle between the perpendicular and

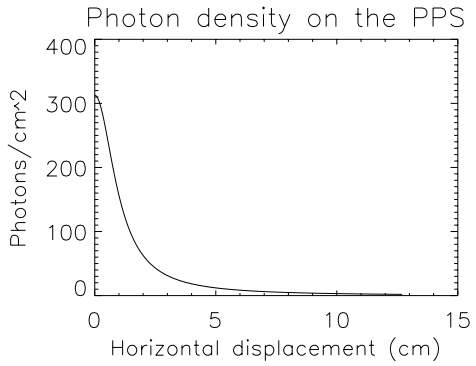

Fig. 3. The photon distribution on the PPSD for 1MeV energy deposited 1 cm from the front face of the PPSD. Total internal reflection is not accounted for in this figure.

the segment connecting the scattering to the point of interest on the PPS. The centroid of this distribution gave a position resolution around 1 mm or less, mostly limited by the statistics of the photon yield. The vertical position was determined from the full-width at half-maximum of the distribution of pixels. This also gave a position resolution of 1 mm. So long as the PPS has sufficiently dense pixelation to not distort the shape of the distributions at the 1 mm level, the detector will have more than enough resolution.

The simulation of the energy collection requires counting the pixels that fired. This technique resembles the spectroscopic tool of "photon counting." So long as the pixels are dense enough to avoid significant pileup, the good energy resolution can be obtained. We estimate that a pixel spacing of 60 to 100 μm is sufficient to preserve the NaI resolution for few MeV hits 1 mm or farther from the PPSD. This yields a pixel pileup probability of 30%. So few pixels sustain this rate of bombardment that this pileup has a small effect. Note that this pixel density is more than enough to preserve the 1 mm position resolution mentioned above.

Energy resolution is normally limited by photon counting statistics. In normal detector geometries there are substantial photon collection losses because the photons fail to reflect from scintillator surfaces or are attenuated within the detector material. The close coupling of the PPS to the thin scintillator will improve our photon collection efficiency substantially. If we were able to detect this many photons, it is possible that we could improve on our estimated 5% energy resolution.

IV. Monte Carlo simulations of the PPSD-based Compton telescope

To make realistic estimates of the response of a Compton telescope constructed using a PPSD we constructed a Monte Carlo simulation of an array of detector elements arranged into a Compton telescope. The simulations were done using GEANT3[4]. These simulations included most of the physics of gamma-ray scattering, including photoelectric absorption and Compton scattering. We assumed that the gamma-rays were normally incident on the center of a 1 m^2 detector, with energies of 0.66 MeV, 1, 2, 3, and 5 MeV.

A. Model detector

Most of the simulations have been made using NaI as the scintillator. The model detector element had a layer of scintillator, a thin PPSD, always assumed to be 1 mm thick borosilicate glass. A small number of simulations included a gap ranging from 0 to 10 cm separating the scintillator elements. The system had as many as 20 elements in it. All detector assemblies were backed by a 20 cm deep NaI scintillator with a PPSD. This last scintillator served the function of guaranteeing a third hit for higher energy incident photons. Also, this scintillator gives us a good chance of completely absorbing the incident photon energy, allowing a measure of the total E. This can be compared with the computed E to determine when to reject the event because of undetected multiple scattering or other effects. All layers were modeled with transverse dimensions of 1 meter by 1 meter.

B. Position determination

A realistic estimate of the position determination was made in this model. In this model, when an interaction occurred, the resulting energy deposit was converted to a photon count (40,000 photons /MeV for NaI, 10,000 photons/MeV for plastic scintillator). The photon count was randomly distributed isotropically within the scintillator. Most of the walls of the scintillator were assumed to be black (absorbing). The remaining photons were spread on the surface of the PPSD in the $\cos^2\theta$ distribution which results from mapping the uniform spherical distribution of photons to the plane. The centroid of the distribution determined the (x, y) position of the hit, and the width of the distribution is determined by the z (distance from the PPSD). The distribution typically yielded a position determination accurate to less than 1 mm in all dimensions.

C. Methodology

Each simulation was run for 200,000 incident gamma-rays. For each incident gamma, the location of each interaction was recorded, along with the energy deposited and the nature of the interaction. For each succeeding interaction, the same information was recorded, until the gamma-ray was absorbed in a photoelectric event or left the detector. The position and energy information was used to estimate a distribution of scintillation photons, then compute the measurable position. The sequence of the hits and the apparent energy and position were used to compute the incident energy and first Compton scattering angle, ϕ_1. We did not implement an algorithm to determine the direction of the source. All the information we would need for that determination was in the first Compton scattering angle, so we worked on evaluation of the precision of that calculation.

D. Results of the Simulations

The basic results of the simulation can be used to demonstrate the good energy and angle resolution of a PPS-based detector, as well as to examine alternative designs of the Compton telescope. Table 2 is a summary of the interesting results of the simulations. These results are not complete. Some studies were directed at answering particular questions, such as the effect of gap size on the resolution of $\delta\phi$, so no attempt was made to include all the efficiencies.

1) Angular Resolution: By resolution, we mean the ability of the detector, scintillator+PPS combination, to resolve two nearby sources. In the case of angle measurements, this resolution characterizes the ability of the detector to identify two sources close to each other in angle.

The angular resolution presented in Table 2 is the full-width half-maximum (FWHM) of the distribution of angles which we calculate from the three-Compton formula.

Figure 4 displays the typical angular resolution from these simulations. Notice that the distribution is more Lorentzian than Gaussian. We examined the efficiency of the detector for different accepted ranges of ϕ_1. These efficiencies are given in Table 2 in the columns Eff (1.5×FWHM), where the gate is put at 1.5× the FWHM of the distribution, and Eff(40mr) where the gate is ±40 mr. A substantial number of events lay outside these gates. The non-Gaussian shape of the distribution has been observed by others simulating the performance of Compton telescopes[5].

To understand the distribution of angles, we plot in Figure 5 the distribution of the measured positions around the true position, in this case for the first and second scatterings from 1 MeV photons. The distribution of measured x appears to be Gaussian. Apparently the Lorentzian distribution of $\delta\phi_1$ arises from the non-linear relationship between the position and the computed Compton angle. The position resolution, from the plot and Table 2, is 1 mm or better.

The angular resolution does not directly imply the precision with which a detector can pinpoint a single source. For a reasonable resolution and a well isolated source, the precision can be improved by adding more statistics, using our high efficiency. Identification of the angle of a particular source with this detector, the angular precision, is better than the apparent resolution, because that is determined by our ability to estimate the centroid of the distribution, which we can do significantly better than the width, depending on our statistics.

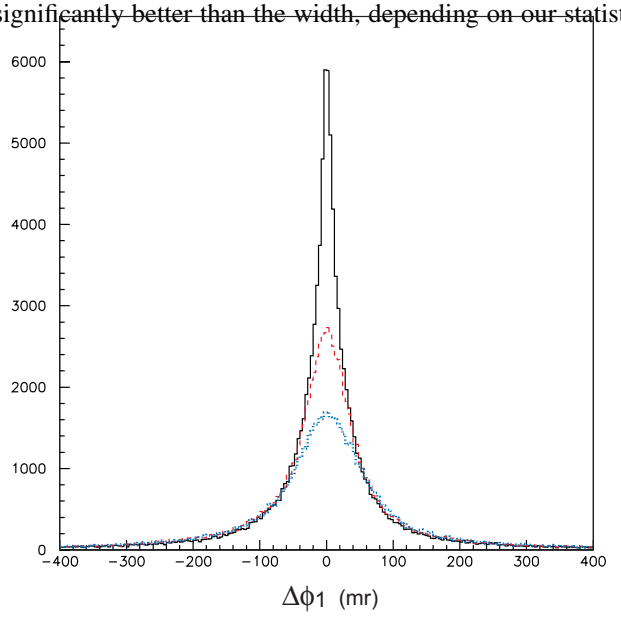

Fig. 4. Angle spectrum for three energies. The solid curve is 5 MeV, the dashed curve is 1 MeV, and the dotted curve is 0.66 MeV. The ordinate is the number of counts in each channel. The abscissa is the difference between the estimated and the true ϕ_1. The difference in the central heights of the curves results from the differing efficiency for detection of the γ-rays, especially the different rates of Compton scattering, and the larger spread in the angle estimates for lower energy γ-rays.

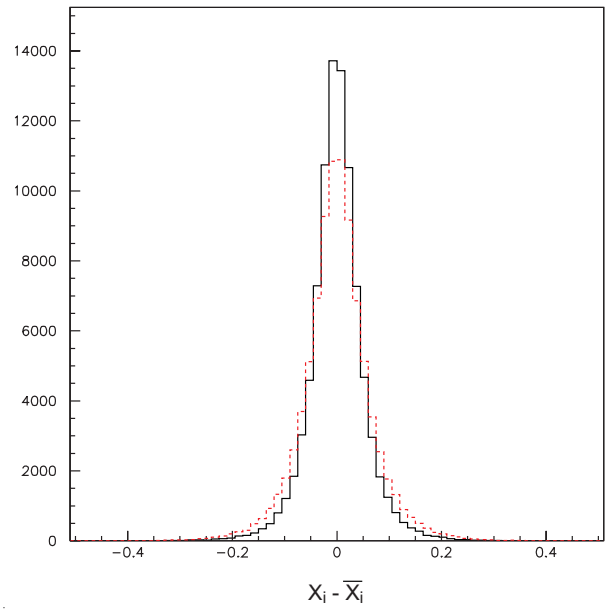

Fig. 5. Distribution of position estimates for 1 MeV gamma-ray incident. The solid curve is position of the first scattering, the dashed curve is the position of the second scattering. The abscissa is the difference between the estimated position and the true position in centimeters. The apparent Lorentzian distribution has been observed by others[5]

TABLE II

SUMMARY STATISTICS OF THE MONTE CARLO SIMULATIONS. EFF(TOTAL) IS THE TOTAL EFFICIENCY, EFF(1.5×FWHM) IS THE EFFICIENCY IF WE COUNT ONLY EVENTS WITH ϕ WITHIN 1.5 TIMES THE FWHM OF THE CENTROID, AND EFF_{40mr} IS THE EFFICIENCY WITH ϕ LIMITED TO ± 40 MR AROUND THE CENTROID OF THE ϕ DISTRIBUTION. ALL DETECTOR ELEMENTS ARE 1 M X 1 M IN TRANSVERSE DIMENSIONS.

Layer (cm)	# layers	E_0 MeV	Eff total	Eff 1.5×FWHM	Eff (40 mr)	Prob (1-hit)	Prob (2-hit)	$\delta\phi$	δx
NaI gap=0									
0.5	20	0.66	0.360	0.279	0.220	0.141	0.0198	6.322	0.044
0.5	20	1	0.435	0.239	0.149	0.117	0.0136	4.560	0.026
0.5	20	5	0.526	0.267	0.311	0.092	0.0085	1.977	
1	10	0.66	0.377	0.243	0.153	0.244	0.0596	6.632	0.110
1	10	1	0.448	0.277	0.214	0.211	0.0443	4.788	0.076
1	10	2	0.460	0.246	0.258			2.718	0.042
1	10	3	0.471	0.244	0.271			2.232	0.035
1	10	5	0.528	0.256	0.307	0.168	0.0281	2.108	0.047
2	5	0.66	0.384			0.361	0.1300	7.367	
2	5	1	0.456	0.361	0.286	0.287	0.0826	5.242	
NaI gap=5cm									
1	10	0.66	0.365					5.848	
1	10	1	0.427					4.008	
1	10	5	0.506					1.811	
NaI gap=10cm									
1	10	0.66						6.253	
1	10	1	0.347					4.064	
1	10	5	0.445					1.690	
Plastic scintillator									
1	20	1				0.085	0.0073	9.058	0.136
2	10	1	0.405			0.172	0.0297	9.399	0.188
2	10	0.66	0.435			0.184	0.0338	13.344	0.240
2	10	5	0.234			0.081	0.0065	2.710	0.072

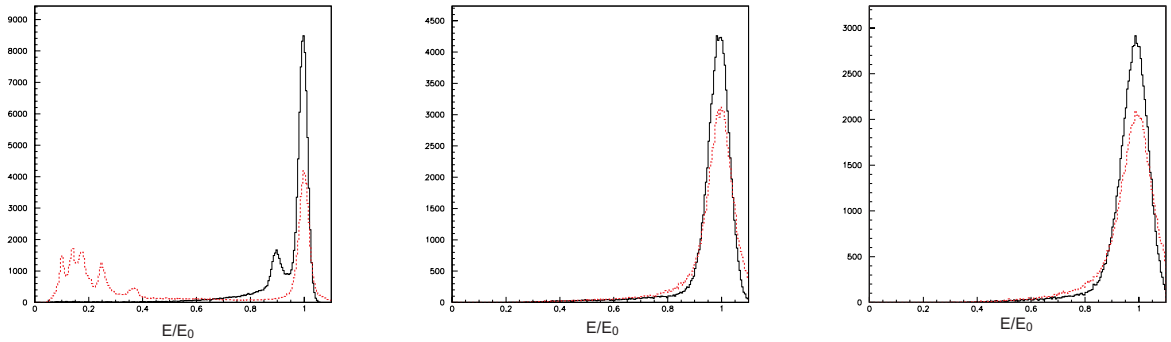

Fig. 6. Energy response, scaled to incident energy for three energies of incident photons. The solid curve is the response of the "sum energy", in which the energy deposited in the scintillators is summed to get the incident photon energy. The dashed curve is the distribution of energies calculated from the Compton scatter events. The plots, from left to right, are for 5 MeV photons, 1 MeV photons and 0.66 MeV photons.

2) Energy Response: The energy response of the model is shown in Figure 6. In each figure the spectrum is normalized to the incident photon energy, so the sum energy peak is near 1.0. The sum energy and Compton energy have similar FWHM and centroids, although the Compton-calculated curve has a high-energy tail. This probably results from the dependence of the algorithm on the angle ϕ_2, which is calculated from the measured positions of the scattering. The positions have a distribution which is symmetric, not constrained by energy conservation. In the case of the 5 MeV spectrum of Figure 6, the low-energy peaks are from photons which escape the detector after only one or two interactions.

A test of the proper functioning of the simulation is to examine the energy of the first and second scattering. Figure 7 illustrates this for 1 MeV phototns. The solid curve is the energy deposited in the first scattering. This resembles the well-known Compton energy distribution, relatively flat as a function of energy with a threshold below the incident energy. The dashed curve is the energy spectrum from the second scattering. Its shape is very different from the Compton-scattering profile and is unexpected, until we realize that the first scattering takes a peak and spreads it uniformly among energies below the Compton threshold. The second scatter takes the Compton profile and spreads it again to lower energies, which now biases the spectrum to low energies.

E. Model design evaluation

In addition to demonstrating the resolution properties of a Compton telescope with PPS readout, we used the simulation to examine some simple optimizations of the design. The simple parameters to examine are the size of the gap and the number of layers on the angle resolution.

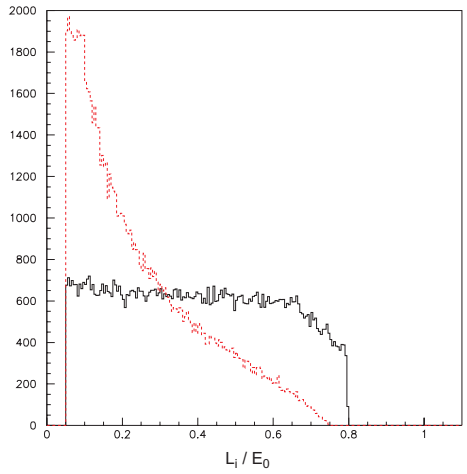

Fig. 7. Energy response for the first Compton scatter, solid curve, and the second Compton scatter, the dashed curve. The incident energy is 1 MeV.

The angular resolution is seen in Figure 8 to be a strong function of energy. At 1 MeV incident, the width of the angle distribution is almost 5°. By 3 MeV it is almost 2° and it does not improve with increasing energy. The improvement in angular resolution in this energy range is a result of the increased energy deposited in each Compton scatter, particularly in the second scattering. Interestingly, although a larger gap should give a better estimate of the angle ϕ, it does not substantially improve $\delta\phi$. Clearly, the excellent position resolution a PPS provides is dominated by the light output of the scintillator, that is, the energy resolution, in calculating the Compton scattering angle. The design with no gap is mechanically superior.

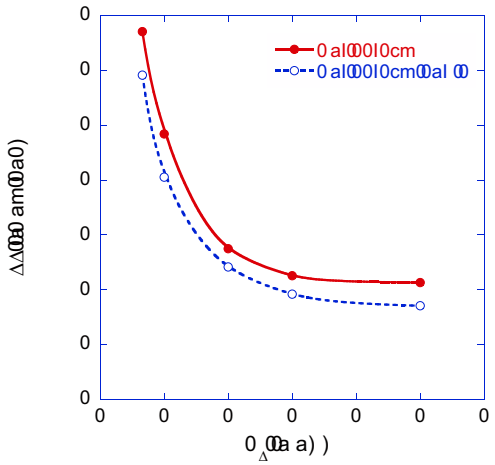

Fig. 8. Width of the distribution of the calculated Compton scattering angle. To produce the "gap" curve, we inserted gaps between the scintillator elements, enlarging the offset between measured points for better angle determination.

The next optimization of the detector design is the choice of a number of layers. Additional layers, as discussed in the next paragraph, increases the efficiency of the detector, but only improves $\delta\phi_1$ by improving the localization of the third scattering. As previously discussed, the detector is limited by the energy resolution of the second scattering, which is not significantly improved by adding layers.

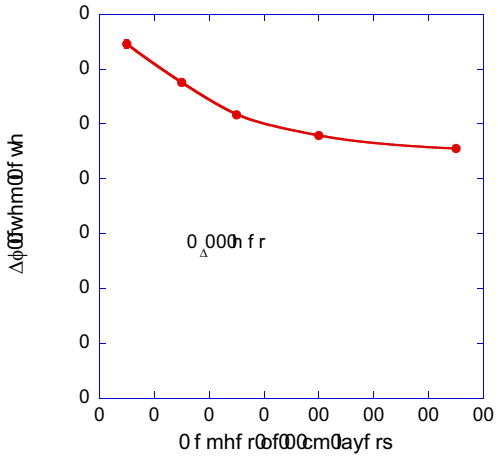

Fig. 9. Angular *resolution* as a function of the number of layers for a 1 MeV gamma ray. This resolution determines our ability to distinguish adjacent sources by angle using the Compton array. Our *precision* for determining the angle of an isolated source is mostly limited by the number of gamma-rays.

Figure 10 demonstrates that adding layers to the detector clearly improves our efficiency. It gives each photon more chance to scatter three times. The total efficiency of the detector reaches nearly 60% for 15 cm thickness. It would require half again as many layers to approach 95%, if there were no other limiting factors. If we only accept tracks with angles within 40 mr of the centroid of the angle distribution, the efficiency drops by half.

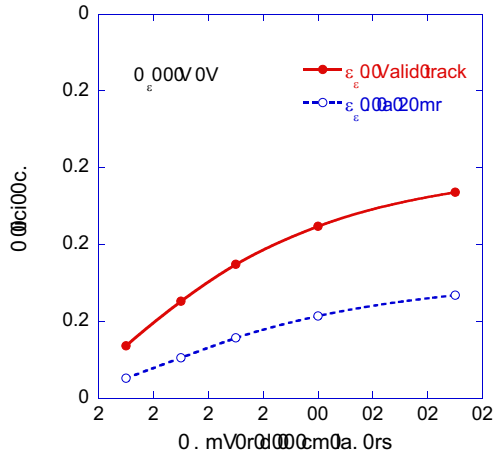

Fig. 10. Detection efficiency as a function of number of layers. Curves are for the total efficiency and the angle-constrained efficiency.

V. Importance of the PPSD to the Compton Telescope

We estimated the performance of a Compton telescope built from layers of scintillator and ideal PPSD detectors. We began with simple estimates of interactions from gamma-ray linear attenuation coefficients and were greatly refined using GEANT3[4]. These simulations were performed at energies of 0.66MeV, 1MeV, 3MeV and 5 MeV, representative of the

range of γ-rays of interest in many applications. The model we settled on used NaI as the scintillator material, with layers of 1cm of NaI each coupled to a PPS (1mm thick) with 10 layers, to give 11 cm total thickness. The model also had a 20 cm thick NaI layer, also coupled to a PPSD at the back of the telescope . At these energies, the model detector had a total efficiency of 45% to 55%, angle constrained efficiencies of 25% to 30%. The angle resolution varied from 6.6° to 2.1°, while the position resolution varied from 1 mm (0.66 MeV) to 0.5 mm (5.0 MeV). For the range of angular resolutions we found in the simulations, it should be straightforward to achieve angle precision of much better that 2°.

We investigated plastic scintillator, but the extra thickness and lower light yield of plastic is a problem. Further work is needed to optimize plastic scintillators and to explore a hybrid of plastic and inorganic scintillators.

Our studies using the Monte Carlo model show that adding extra gaps to space the detector elements does not improve the angular resolution. Detector elements which were thinner or thicker did not show significant differences, either.

The PPS offers a means to obtain position resolution using scintillation detectors that is comparable to that now available using Ge and Si detectors. A fully developed PPS can revolutionize any detection system in which position measurements with small detector mass and large area are critical. Beyond the application examined here, it can revolutionize medical tomography and high-energy neutron research.

Many more investigations are needed to optimize the design. We have not investigated threshold effects in the telescope, nor have we investigated the effect of background photons on the response. We can investigate the thickness of the detector layers, the effects of backscattering, multiple scattering within a layer, and the effects of optical photon pileup. Further investigations will examine alternative scintillators, with lower Z to enhance Compton scattering over photoelectric absorption and greater brightness to improve our resolution. We believe that hybrid detectors, composed of a mix of scintillators, may prove to have the best performance.

REFERENCES

[1] P. S. Friedman, "Plasma Panel Sensors as Scintillation Detectors", IEEE NSS-MIC, San Diego (Nov 2006), Paper N30-136.

[2] J.D. Kurfess, W.N. Johnson, R.A. Kroeger, and B.F. Phlips, "Considerations for the Next Compton Telescope Mission", in The Fifth Compton Symposium, ed. M.L.McConnell and J.M. Ryan, AIP Conf Proc. 510, 2000.

[3] Hubbell, J.H. and Seltzer, S.M. (2004), Tables of X-Ray Mass Attenuation Coefficients and Mass Energy-Absorption Coefficients (version 1.4). [Online] Available: http://physics.nist.gov/xaamdi [2007, October 12]. National Institute of Standards and Technology, Gaithersburg, MD. Originally published as NISTIR 5632, National Institute of Standards and Technology, Gaithersburg, MD (1995).

[4] R. Brun et al., GEANT3, CERN Report No. DD/EE/84-1 1987.

[5] Sudhakar Chelikani, John Gore and George Zubal, Phys. Med. Biol. 49 (2004) pp 1387-1408.